A Novel Pore Structure Tortuosity Concept Based on Nitrogen Sorption Hysteresis Data

Constantinos E. Salmas and George P. Androutsopoulos*

Department of Chemical Engineering, Section II, Chemical Process Engineering Laboratory, National Technical University of Athens, 9 Heroon Polytechniou Street, GR 15 780 Athens, Greece

A corrugated pore structure model (CPSM−nitrogen)[9] was employed to define a novel pore structure tortuosity concept. An empirical correlation is proposed for the prediction of tortuosity factors τ_{CPSM} as follows: $\tau_{CPSM} = 1 + A[(D_{max,eff} - D_{min,eff})/D_{mean}](N_S - 2)^a$. Constants A and a are adjustable parameters. The second factor reflects the influence of the intrinsic pore size distribution, and the third expresses the contribution of the nominal pore length parameter N_S. The latter is, by definition, the number of pore segments forming a single corrugated pore of the CPSM pore configuration model and represents the frequency of pore cross section variation per unit length along a characteristic catalyst pellet dimension. The determination of N_S and $(D_{max,eff} - D_{min,eff})/D_{mean}$ is accomplished by fitting the CPSM model over the pertinent nitrogen sorption hysteresis data. Coefficients A and a were found to be $A = 0.69$ and $a = 0.58$ by applying the empirical correlation for two specified materials of known tortuosity. The tortuosity factors for an anodic aluminum oxide membrane, MCM-41 materials, dried lignite, a porous glass, and several HDS catalysts were predicted to be 2.60, 1.12−1.13, 1.33−2.79, 6.60, and 2.75−10.07, respectively. Such values approximate the literature data. Mercury porosimetry runs on the HDS catalysts showed a proportional increase in mercury entrapment with an increase in the corresponding τ_{CPSM} values. The tortuosity factor of lignite increases proportionally with the pore volume evolution. Further testing of the proposed correlation requires a rigorous analysis of diffusion phenomena, based on the CPSM pore structure configuration, combined with effective diffusivity measurements.

Introduction

Pore structure tortuosity has been the subject of numerous publications dealing with studies of diffusion through porous media. A comprehensive review of earlier literature is given in ref 1, which includes an extensive tabulation of experimentally determined values of tortuosity factors valid for a variety of catalysts. A quite recent review[2] of published work provides information for hindered or restricted diffusion in liquids contained in fine porous materials.

The majority of communications on diffusion through porous solids concern the diffusion of gases through a pore system and, particularly, the correlation of effective diffusivity with the respective binary diffusion coefficient D_b. The most popular correlation involves the voidage fraction (ϵ) and a pore tortuosity factor (τ). Thus

$$D_e = D_b\epsilon/\tau \qquad (1)$$

This is a convenient tool, especially for those measuring effective diffusivities using a Wicke and Kallenbach cell or an equivalent experimental setup. The tortuosity factor τ is an overall index of the intricate pore structure, and its evaluation from eq 1 becomes possible if the D_e, D_b, and ϵ values have been measured or calculated from established correlations. Traditionally (e.g., Petersen,[3] Michaels[4]), there have been attempts to attach physical insights to the factor τ in terms of a concrete pore geometry that involves pore cross section irregularities and a pore length parameter. Pore cross-sectional area variation is also termed the "shape factor" (S) and is related to the ratio of the maximum to the minimum pore cross sections. The pore length parameter (L) is also called the "angle factor", i.e., the pore axis deviation from the main straight diffusion direction (considered unidirectional). Because these two parameters cannot be distinguished for most real porous solids, they are usually multiplied together and represented by τ the tortuosity factor, which lumps together the pore length and pore cross section variation effects. For accurate work, τ must be determined experimentally (Satterfield).[1]

For the case of restricted diffusion of species through a liquid phase contained in pores, eq 1 includes an additional factor $F(\lambda)$. Thus

$$D_e = (D_b\epsilon/\tau)\, F(\lambda) \qquad (2)$$

$F(\lambda)$ is considered to be a restrictive factor (≤ 1) that accounts for the interaction of the solute molecular size and the pore size. Variable λ is the ratio of the solute critical molecular diameter to the pore diameter (i.e., $\lambda = d_s/d_p$). When the solute size is relatively small compared with the pore size, $F(\lambda) = 1$. Various empirical expressions for $F(\lambda)$ have been reported, viz., $F(\lambda) = (1 - \lambda)^z$ (Beck and Schultz)[5] and $F(\lambda) = e^{-b\lambda}$ where $b = 4.6$ (Satterfield et al.).[6] Tortuosity factor τ can be calculated from eq 1 when D_b, D_{eff}, ϵ, and $F(\lambda)$ are known.

Furthermore, $F(\lambda)$ weights for the restrictive effects due to interactions between the solute molecular size and the pore size, whereas τ is exclusively related to pore size distribution and the pore geometry characteristics of the material under examination. Experimental

* Corresponding author. Tel.: (+301) 772 3225. Fax: (+301) 772 3155. Email: androuts@orfeas.chemeng.ntua.gr.

10.1021/ie000626y CCC: $20.00
Published on Web 12/20/2000

determination of effective diffusivities D_{eff} can be implemented by carrying out combined adsorption−equilibrium and diffusion runs either in a diffusion cell[6] or in a stirred tank reactor.[7] These measurements lead also in estimates of τ and the validation of a correlation for $F(\lambda)$.

It is evident from the foregoing introduction that the pore structure plays the key role in the elucidation of diffusion phenomena. As pointed out by Petersen,[3] there has been no satisfactory experimental data, at the time of his work, to characterize the structure of pores in compacted materials in a way that allows for a sensible application of his theory of diffusion through a periodically constricted pore model. The lack of suitable porosimetry information also led Michaels[4] to conclude that simplified capillary models, because of their idealized nature, do not provide for refinements regarding the understanding of the diffusion process through a porous medium.

Tortuosity Factor Predictions from Porosimetry Measurements. A first attempt to predict tortuosity factors by using porosimetry information without the execution of diffusion measurements was made by Carniglia.[8] An empirical relationship was proposed that correlates the tortuosity factor of a specific material with mercury porosimetry data as well as other pore structure characterization properties. Pore volume, BET surface area, particle bulk density (Hg), pore size distribution data, and a pore shape parameter are required for the evaluation of tortuosity factors by the Carniglia model. He reported a fair agreement between tortuosity factors computed with his method and those calculated from diffusion measurements for a variety of metal oxides and catalysts.

However, the model is of an approximate nature. One possible drawback is related to the fact that the mercury porosimetry (MP) method cannot reliably trace pore sizes in the lower mesopore region, i.e., 2−3.7 nm, despite the fact that the relevant BET data involve pore sizes in this range. Furthermore, the hysteresis and entrapment effects inherently present in MP intrusion−extrusion measurements might also introduce uncertainty as they disguise the true picture of the intrinsic pore volume distribution. Thus, the mean pore sizes to be used in applying the model might deviate appreciably from the most representative mean value.

The scope of the present study is to develop (i.e., formulate and apply) a simplified empirical correlation for the prediction of tortuosity factors τ_{CPSM} based on nitrogen sorption hysteresis data as described by the fitting parameters of a corrugated pore structure model (CPSM).[9] The CPSM theory enables the evaluation of the intrinsic distribution of pore structure properties as well as that of the characteristic pore length parameter N_S.

Corrugated Pore Structure Model (CPSM). The corrugated pore structure model (CPSM-nitrogen) is currently under development.[9,10] It is a statistical model simulating the gas adsorption and capillary condensation−evaporation phenomena that produces a single psd prediction by curve-fitting the entire sorption hysteresis loop and is based on a corrugated pore concept. The latter is envisaged to be composed of a sequence of N_S cylindrical pore segments of a constant length and distributed diameter. Figure 1 illustrates how the overall CPSM configuration results from the classical pore model made up of an array of parallel cylindrical pores of distributed size. The development of the CPSM-nitrogen model is based on a number of assumptions:[9] (1) The physical multilayer adsorption on the surface of the corrugated pore is described by a modified Halsey equation (Appendix eq I-1). (2) Capillary condensation occurs according to the Kelvin equation (Appendix eq I-2). (3) The condensation is assumed to commence on a cylindrical interface at the narrowest segment and at a later stage proceeds through a hemispherical one, whereas evaporation proceeds preferably through a hemispherical interface geometry.

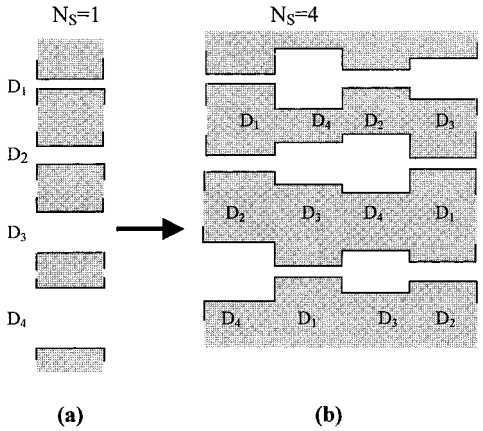

Figure 1. Schematic illustration of the corrugated pore model construction. (a) Conventional pore model made up of a statistically large number of cylindrical pores of distributed size [i.e., according to $F(D)$]. (b) Corrugated pores formed by combining randomly (e.g., in groups of four) the pore segments comprising model a.

Following a statistical analysis of the envisaged physical steps taking place within the corrugated pore, the pertinent formulas have been derived.[9] CPSM final equations are presented in Appendix eqs I-3−I-5. To facilitate the practical application of the CPSM model in the evaluation of tortuosity factors, a family of bell-shaped distribution functions (BSDs) was chosen as the intrinsic pore number distribution $f_r(b_r,D)$ (Appendix eq I-7). The respective intrinsic pore number distribution $F(D)$ (eq I-6) appearing in the CPSM model equations can be derived by combining a set of n f_r-type psds. The mathematical formula of the BSD enables the analytical integration of the CPSM model, which thus becomes a flexible analytical tool to be used for the prediction of intrinsic pore size distributions.

The corrugated pore configuration has been used in simulations of mercury porosimetry (MP) hysteresis[11] and investigations of MP hysteresis loop scanning that enable the definition of pore structure tomography concepts.[12,13]

Theory

Pore Structure Tortuosity Factor (τ_{CPSM}) Definition. The geometric characteristics of the general corrugated pore offer a sound basis for the definition of a new tortuosity factor. Use is made of N_S and the intrinsic pore size distribution (psd) function $F(D)$, defined over a range $D_{min}-D_{max}$ of pore sizes. Pore tortuosity can be seen as dependent upon the frequency of pore diameter variation per unit length of the characteristic particle dimension. The pore diameter variation is denoted by the value of N_S (a measure of a nominal pore length) that can be considered as the pore

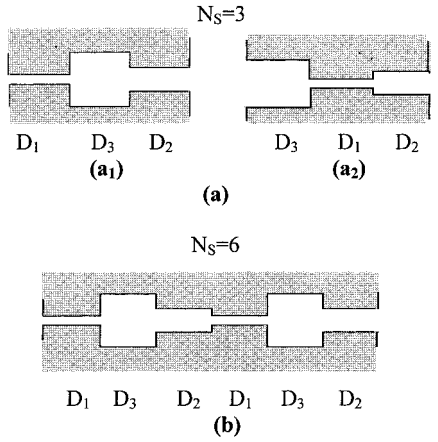

Figure 2. Effect of N_S on pore tortuosity. By increasing N_S [i.e., (a) $N_S = 3$, (b) $N_S = 6$] with other pore structure parameters held constant [i.e., the intrinsic $F_V(D)$, $V_{p(a1)} + V_{p(a2)} = V_{p(b)}$, and $D_{max} - D_{min} = D_3 - D_1$], pore tortuosity increases.

geometry deviation from an absolutely cylindrical shape. In classical terminology N_S can be seen as the "pore length parameter" or the angle factor. It can also be seen as dependent upon the extent of pore cross-section variation. Pore cross-sectional area variation between neighboring segments increases as the range D_{min}—D_{max} becomes wider. More precisely, the degree of pore irregularity is expressed by the intrinsic pore size distribution. In conventional terms, this parameter represents the shape factor.

Effect of Parameter N_S on Pore Tortuosity. The simplified configuration of corrugated pores appearing in Figure 2 illustrates that the pores of Figure 2a have a total pore volume and surface area equal to those of the pore in Figure 2b. They also have identical D_{min} D_{max} values and are differing in the number of segments per corrugated pore. All pores of Figure 2 involve the same pore segment sizes, i.e., D_1, D_2, and D_3. The definition of tortuosity τ to be introduced in this work assumes that the pores shown in Figure 2b are more tortuous than those of Figure 2a. Thinking in terms of porosimetry, structure b is anticipated to cause intense hysteresis phenomena associated with either nitrogen capillary condensation—evaporation or even mercury penetration—retraction phenomena.

Real pore structures exhibiting identical intrinsic pore size distribution $F(D)$ but differing in the value of N_S are expected to be characterized by different tortuosity factors.

Effect of ($D_{max} - D_{min}$) on Pore Tortuosity. The width of the pore size range, over which the pore size distribution extends, is to be related to pore structure tortuosity. To demonstrate this phenomenon in terms of a single corrugated pore, consider the pore configurations of Figure 3a—c.

Pore configuration a is expected to give rise to intense hysteresis phenomena (e.g., nitrogen or mercury porosimetry). The latter phenomenon seems to be relaxed as the pore structure complexity progressively transforms to pore types b and c. Indeed by reducing the difference ($D_{max} - D_{min}$), pore uniformity increases, and the pores become less tortuous. From the foregoing discussion, it becomes obvious that the formulation of a correlation for the prediction of tortuosity factors should be the combined effect of two factors, i.e., N_S and ($D_{max} - D_{min}$). Both parameters can be evaluated by following an analysis of porosimetry data based on the

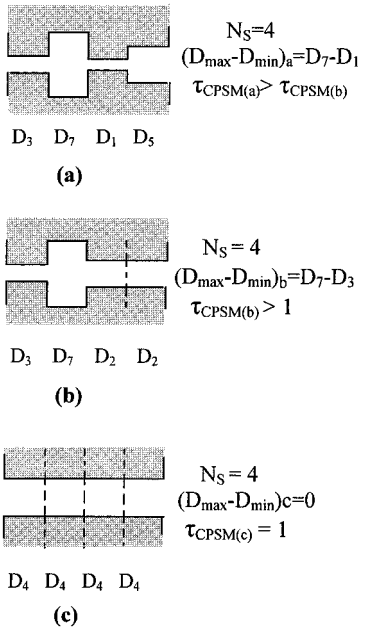

Figure 3. Single corrugated pore configurations of differing tortuosities τ_{CPSM}. Constant pore volume (i.e., $V_{pa} = V_{pb} = V_{pc}$), same number of segments per pore (i.e., $N_S = 4$). (a) $V_{pa} = V_1 + V_3 + V_5 + V_7$, (b) $V_{pb} = 2V_2 (= V_1 + V_5) + V_3 + V_7$, (c) $V_{pc} = 4V_4 (= V_1 + V_3 + V_5 + V_7)$. By decreasing ($D_{max} - D_{min}$) in the order $(D_{max} - D_{min})_a > (D_{max} - D_{min})_b > (D_{max} - D_{min})_c$, pore tortuosity is reduced.

corrugated pore structure model (CPSM). The presentation of the relevant formulas and applications for porous materials will be provided in following paragraphs.

Combined Effect of N_S and ($D_{max} - D_{min}$) on τ_{CPSM}. As discussed in the foregoing paragraphs, the tortuosity factor τ_{CPSM} becomes higher as both N_S and ($D_{max} - D_{min}$) assume higher values. It is also imperative that $\tau_{CPSM,min} \rightarrow 1$ for the simplest possible pore structure composed of independent, straight, parallel cylindrical pores of distributed size (e.g., Figure 3c). In terms of a single corrugated pore, this should be true either for ($D_{max} - D_{min}$) $\rightarrow 0$ and any value of N_S or for $N_S \rightarrow$ its minimum value (i.e., $N_S = 2$) and any value of ($D_{max} - D_{min}$). The dependence of τ_{CPSM} on N_S should ensure that τ_{CPSM} assumes reasonable values compared with those obtained from diffusion measurements. For instance, the correlation to be developed should predict very low τ_{CPSM} values for simple and regular (prototype) pore structures, e.g., the structure of either MCM-41 materials[14–17] or anodic aluminum oxide films composed of straight, independent pores with more or less constant pore cross-sectional areas. Similarly, the τ_{CPSM} predictions should be in a satisfactory agreement with experimental τ values for a variety of porous materials that evidently possess a complex pore structure.

Definition of a Tortuosity Factor in the Context of the CPSM Model. The analysis of porosimetry hysteresis data in terms of the CPSM theory aims at the evaluation of two crucial pore structure parameters, i.e., the intrinsic psd and the pore length parameter N_S. Such pore structure data might find a useful application in the classification of porous solids as regards their pore structure complexity. A definition of a new pore structure tortuosity factor takes account of the CPSM simulation data. The new tortuosity factor, τ_{CPSM} (eq 2) , bears the conventional meaning as regards the diffusion process envisaged to occur though the porous material under examination. The physical significance

Table 1. CPSM Fitting Parameters Referred to Hysteresis Loops of Figure 4

material code	$V_{g,max}$[a,b]	N_S[c]	parameters of the intrinsic pore segment number distribution $F(D)$						P_{ce}/P_0	$(P/P_0)_{max}$	Kelvin parameters[d]		adsorbed gas layer thickness parameters, eq 2	
			b_1	b_2	b_3	w_1	w_2	w_3			$\cos\theta_c$	$\cos\theta_h$	m	n
MCM-41 (novel mesoporous materials)														
Wu et al. 1996	1006.06	2.05	−2450	−600	−15	6.5	1	10	0.270	0.994	1.00	1.00	0.28	0.35
Ravikovitch et al. 1998	949.40	2.10	−1800	−600	−12	6.5	1	5	0.235	0.994	1.00	1.00	0.14	0.45
anodic membranes														
anodic γ-Al_2O_3	0.2368[e]	4.00	−8.30	–	–	1.0	–	–	0.535	0.968	0.75	1.00	0.02	0.28
lignite (partially dried samples)														
run 1 (without drying)	3.88	2.1	−5	−2000	–	105.0	10	–	0.40	0.9980	0.03	0.03	0	0.35
run 2 (drying 100 °C, 1 h)	7.18	3.0	−5400	−530	–	35.0	1000	–	0.25	0.9997	0.45	0.45	0	0.31
run 3 (drying 150 °C, 1 h)	9.84	3.0	−5400	−490	–	35.0	1000	–	0.25	0.9996	0.65	0.65	0.1	0.38
run 4 (drying 200 °C, 1 h)	12.88	3.5	−5400	−558	–	35.0	1000	–	0.25	0.9996	0.65	0.65	0.1	0.35
run 5 (drying 250 °C, 1 h)	8.58	3.2	−5400	−543	–	41.0	1000	–	0.25	0.9996	0.65	0.65	0.1	0.38
run 6 (drying 100 °C, 3 h)	12.14	3.5	−5400	−530	–	36.0	1000	–	0.25	0.9996	0.68	0.68	0.1	0.35
HDS catalysts														
Harshaw HT- 400E	308.1	4.3	−100	–	–	1.0	–	–	0.32	0.990	1.00	1.00	0.100	0.39
Girdler G 51 (3.0 mm)	328.4	4.5	−350	−110.	–	13.0	10	–	0.39	0.995	0.90	0.90	0.150	0.43
Girdler G 51 (1.5 mm)	404.0	3.8	−150	−45	−2.5	15.0	10	7	0.40	0.9912	0.70	0.70	0.150	0.40
ICI 41−6	394.0	4.5	−75	−2.	–	6.0	1	–	0.44	0.990	0.80	1.00	0.170	0.44
Comox 451	304.2	5.8	−70	−15	−1	15.0	10	10	0.40	0.965	0.65	0.65	0.075	0.39
ICI 61−1	344.0	5.5	−90	−5	–	12.0	1	–	0.44	0.990	0.975	0.975	0.180	0.40
H_2-type loop (IUPAC)														
theoretical example [9]	646.4	30	−400	–	–	1	–	–	0.25	0.993	0.8	1.0	0	0.35
porous glass [19]	29.64	60	−200	–	–	1	–	–	0.46	0.99	0.38	0.38	0.09	0.40

[a] Units = cm^3 of N_2 (STP)/g. [b] Sorption data reported in refs 10 and 18. [c] Pore cross section variation number. [d] As defined by eq 11.[9] [e] Units = cm^3 of N_2 (STP)/m^2 of foil.

of τ_{CPSM} is better understood by realizing that τ_{CPSM} is the sum of unity and the product of three contributing factors, as follows:

$$\tau_{CPSM} = 1 + \begin{pmatrix}\text{an adjustable parameter}\\ \text{to relate tortuosity with}\\ \text{a reference pore structure}\end{pmatrix} \times \begin{pmatrix}\text{a factor related to}\\ \text{pore size distribution}\\ \text{characteristics}\end{pmatrix}\begin{pmatrix}\text{a factor related}\\ \text{to the nominal}\\ \text{pore length}\end{pmatrix} \quad (2)$$

The first factor (i.e., A) is an adjustable parameter computed for a reference pore structure of known or assumed tortuosity, the second expresses the contribution of the pore size distribution characteristics, and the third accounts for the frequency (N_S) of pore cross-sectional area variation with respect to unit length in the general direction of diffusion. As explained earlier in this work, it is more appropriate to consider N_S as the nominal pore length of a straight corrugated pore. The following general correlation is proposed for the evaluation of τ_{CPSM}:

$$\tau_{CPSM} = 1 + A\left(\frac{D_{max,eff} - D_{min,eff}}{D_{mean}}\right)(N_S - 2)^a \quad (3)$$

The values of A and a refer to selected (reference) pore structures of known tortuosities. $D_{max,eff}$, $D_{min,eff}$, and N_S are determined through nitrogen sorption porosimetry measurements. D_{mean} is the mean pore diameter of the intrinsic pore volume distribution as predicted by the CPSM model. The effect of psd skewness is taken into account through the use of the D_{mean} in deriving the form of the reduced pore size range.

Definition of $D_{max,eff}$ and $D_{min,eff}$. The values of $D_{max,eff}$ and $D_{min,eff}$ can be obtained via eq 4.

$$\int_{D_{max,eff}}^{D_{max}} F_V(D)\,dD = \int_{D_{min}}^{D_{min,eff}} F_V(D)\,dD = 0.025 \quad (4)$$

$F_V(b)$ is the normalized pore volume distribution function. Taking the pore number distribution function as $F(b;D)$, the pore volume distribution is

$$F_V(b) = D^2F(b;D) \quad (5)$$

Thus, eq 4 is transformed into

$$\int_{D_{max,eff}}^{D_{max}} D^2F(b;D)\,dD = \int_{D_{min}}^{D_{min,eff}} D^2F(b;D)\,dD = 0.025 \quad (6)$$

D_{max} and D_{min} are the values detected by the nitrogen sorption porosimetry measurements. The consideration of $D_{max,\,eff}$ and $D_{min,eff}$ arises from the need to truncate distributions showing long tails that asymptotically approach the pore size axis. The values $D_{max,eff}$ and $D_{min,eff}$ are more realistic than the absolute ones, obtained from the gas sorption porosimetry measurements prior to the psd truncation. The integral value of 0.025 in eq 6, though arbitrary, was chosen to be small so that, by truncating the pore volume psd, a percentage of 2.5% (i.e., 5% overall) of the area is left out on each end of the distribution. Because of the empirical nature of the proposed tortuosity correlation, the truncation margin is sufficiently small and there is no point in optimizing it further.

Evaluation of Parameters *A* and *a*. The evaluation of parameters A and a can be achieved by solving eq 3 for $\tau_{CPSM(1)} = 4.9$ and $\tau_{CPSM(2)} = 6.6$. The first tortuosity value is valid for an HDS catalyst (Comox 451) and has been provided by the catalyst manufacturer (i.e., Laporte Industries Ltd, Widnes Lancashire, U.K.). This value is typical of porous catalysts. The second tortuosity is an average of the values valid for Vycor porous glass materials.[1] CPSM fitting data for the HDS catalyst[9] and a porous glass[19] are displayed in Tables 1 and 2, and the pertinent fitted loops are presented in Figures 4 and 7, respectively. Thus, the application of eq 3 for the materials under consideration yields $A = 0.69$ and $a =$

Table 2. Predicted Tortuosity Factors for Various Categories of Porous Materials

material code	N_S	$D_{min,eff}$ (nm)	$D_{max,eff}$ (nm)	D_{mean} (nm)	τ_{CPSM}	pore volume[a] (cm^3/g)	fractional entrapment[b]
MCM-41 (novel mesoporous materials)							
Wu et al. 1996	2.05	2.272	4.00	2.5354	1.12	1.57	–
Ravikovitch et al. 1998	2.10	2.425	4.4918	2.787	1.13	1.48	–
anodic aluminum oxide membranes							
anodic γ-Al_2O_3	4.0	6.84	36.4	19.09	2.60	3.7[c]	–
lignite (partially dried samples)							
run 1 (without drying)	2.1	1.32	32.96	17.39	1.33	0.006	–
run 2 (drying 100 °C, 1 h)	3.0	3.87	48.12	21.59	2.41	0.011	–
run 3 (drying 150 °C, 1 h)	3.0	4.40	56.01	25.32	2.41	0.015	–
run 4 (drying 200 °C, 1 h)	3.5	4.32	49.80	22.30	2.64	0.020	–
run 5 (drying 250 °C, 1 h)	3.2	3.78	51.10	22.83	2.59	0.013	–
run 6 (drying 100 °C, 3 h)	3.5	4.47	54.60	24.47	2.79	0.019	–
HDS catalysts							
Harshaw HT- 400E	4.3	3.90	18.26	9.17	2.75	0.48	0.32
Girdler G 51 (3.0 mm)	4.5	3.68	25.17	9.12	3.77	0.42	0.44
Girdler G 51 (1.5 mm)	3.8	3.37	129.74	27.46	5.46	0.52	0.44
ICI 41−6	4.5	4.47	126.01	22.20	7.42	0.56	0.73
Comox 451	5.8	2.94	34.25	11.92	4.90	0.41	0.78
ICI 61-1	5.5	4.69	111.00	16.72	10.07	0.53	0.88
H_2-type loop (IUPAC)							
theoretical [9]	30	2.4	6.2	3.7	5.89	1.00	–
porous glass [19]	60	2.46	5.0	3.31	6.60	0.046	–

[a] Determined by nitrogen sorption. [b] Determined by mercury porosimetry. [c] Units are cm^3/m^2 of aluminum foil.

0.58. Hence, eq 3 is transformed as follows:

$$\tau_{CPSM} = 1 + 0.69\left(\frac{D_{max,eff} - D_{min,eff}}{D_{mean}}\right)(N_S - 2)^{0.58} \qquad (7)$$

Equation 7 constitutes the CPSM-tortuosity model and is proposed for tortuosity (τ) predictions of mesoporous materials. Its application requires knowledge of the pertinent sorption hysteresis data and the corresponding CPSM simulation parameters. Further improved estimates of the constants A and a can be pursued via use of additional gas sorption and tortuosity data. However, a more rigorous testing of the proposed correlation should include an analysis of the intrinsic diffusion steps combined with gas sorption porosimetry and effective diffusivity measurements.

Evaluation of Tortuosity Factors. Equation 7 is employed in the evaluation of τ_{CPSM} for various porous materials, e.g., MCM-41 novel mesoporous materials, an anodic aluminum oxide film, a porous glass, partially dried lignite samples, and HDS catalysts. The data needed to apply eq 7 are obtained by fitting the CPSM-nitrogen model over the pertinent nitrogen sorption hysteresis data obtained from refs 10 and 18 for the material under consideration (Figure 4). The simulation has been performed assuming a composite bell-shaped distribution function (composite BSD) that accounts for the pore volume distribution function according to eqs I-6 and I-7 (Appendix). As shown in Figures 4 and 7b, the fitting of experimental points for each one of the materials studied has been quite successful. The relevant CPSM fitting parameters are provided in Table 1. The data required to apply eq 7, together with computed τ_{CPSM} values, are summarized in Table 2. However, it should be noted that the pore diameters estimates (Table 2) for the MCM-41 data reported in ref 14 (Figure 4, Wu et al., 1996, plot) were obtained from the corresponding pore volume distribution of Figure 5. Mistakenly, the latter figure was omitted from ref 10.

Discussion

As already presented in previous paragraphs, two major pore structure properties are incorporated in the CPSM-tortuosity model. Also as already presented in previous paragraphs, two major pore structure properties are incorporated in the CPSM-tortuosity model.

The first, named the *frequency of pore diameter variation per unit length of a characteristic particle dimension*, can be thought of as a *nominal pore length* parameter of the material under consideration. This parameter is equivalent to L as described in the Introduction section and accounts for the longer distance that a diffusing molecule has to travel than the straight distance between two fixed points within a porous particle. This length parameter is also known as the angle factor because diffusion paths longer than the corresponding shortest path imply that a pore axis deviates from the main straight diffusion direction. In CPSM terms, the pore length parameter is expressed by N_S, the nominal pore length of the general statistical corrugated pore. Evaluation of N_S can be achieved by carrying out CPSM-nitrogen simulations of nitrogen sorption hysteresis data. In this respect, the CPSM-tortuosity model employs the CPSM-nitrogen model[9,10] as its theoretical background.

The second pore structure parameter involved in the CPSM-tortuosity model is that related to the *extent (severity) of the pore cross-sectional area variation*. Traditionally, this parameter is called the pore shape factor, i.e., S, and is related to the ratio of the maximum to the minimum pore cross section. In the CPSM-tortuosity model, this factor is expressed by a dimensionless pore size distribution width deduced from the intrinsic pore volume psd data. Intrinsic psd data are computed by applying CPSM-nitrogen simulations of nitrogen sorption hysteresis data. This is also a case where the CPSM-nitrogen model constitutes the theoretical background of the CPSM-tortuosity model.

From the foregoing discussion, it is concluded that the CPSM-tortuosity correlation includes the product of two distinct factors, pore length and pore shape, that can

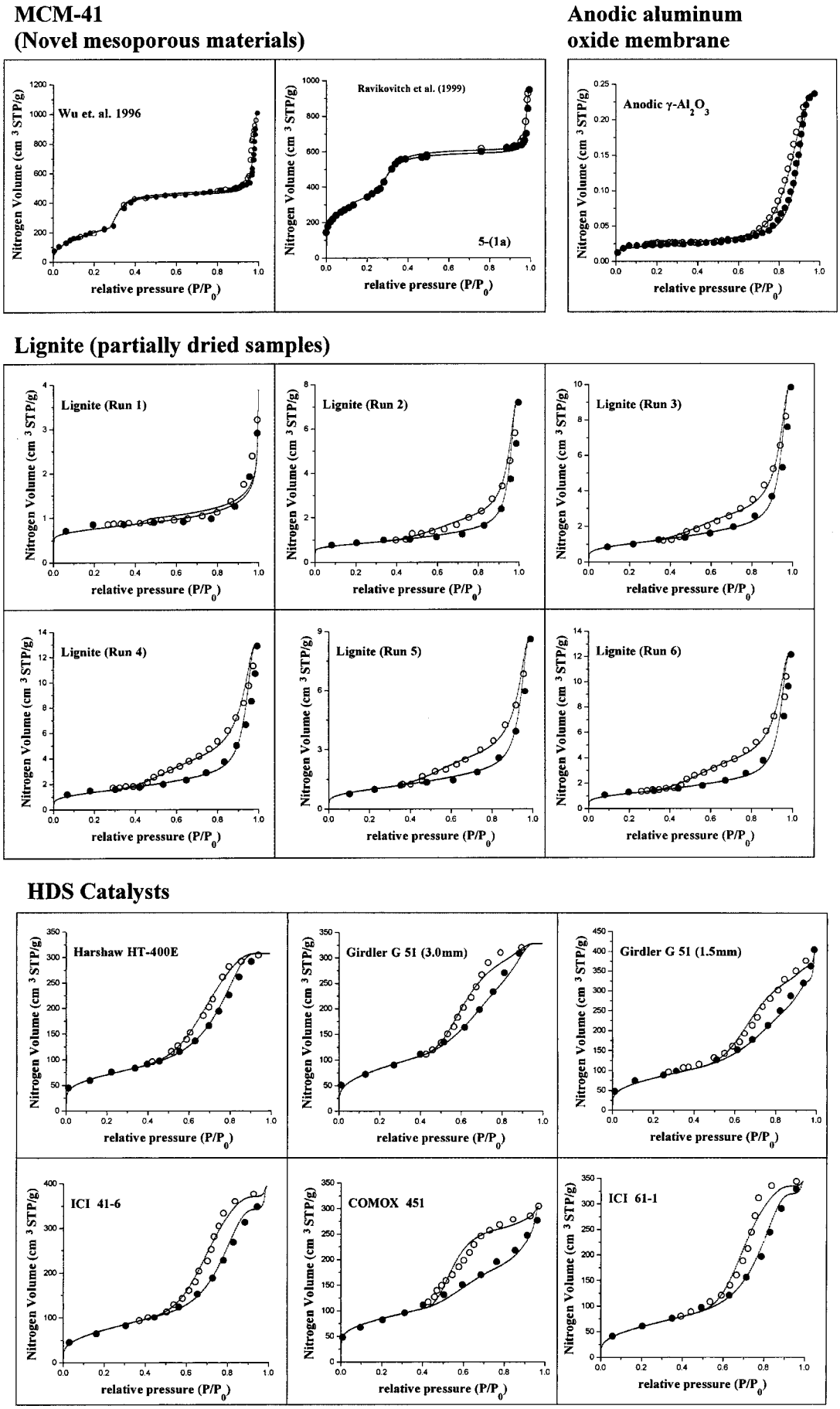

Figure 4. Nitrogen sorption hysteresis data for four categories of porous materials.[10,18] ●, Adsorption−capillary condensation data. ○, Desorption−capillary evaporation data. Solid line, CPSM model regression result. CPSM fitting parameters are provided in Table 1.

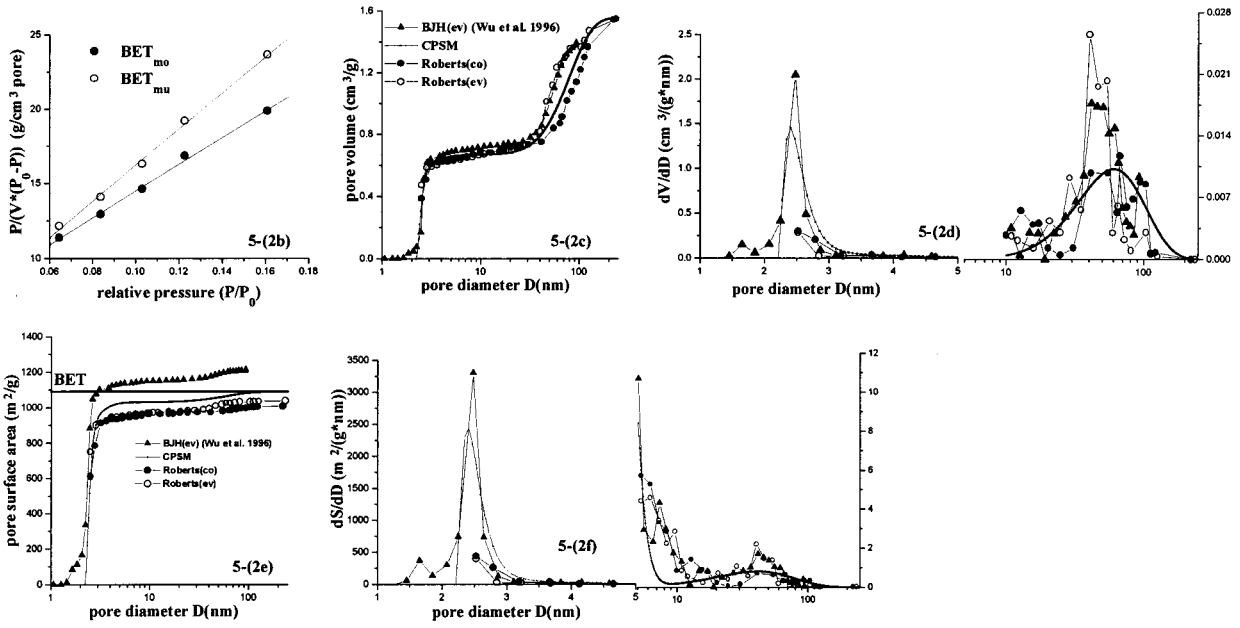

Figure 5. Intrinsic pore size distributions and surface area plots for an MCM-41 material. Sorption data are reported in ref 14. CPSM-nitrogen simulation parameters are reported in Table 1 (i.e., Wu et al.).

be determined by employing the CPSM-nitrogen model in simulations of nitrogen hysteresis data. This direct connection between pore tortuosity and porosimetry measurements is a new development. A similar work based on mercury porosimetry data is that reported in ref 8. Relevant comments concerning the latter method have already presented in the Introduction section of this work.

To further develop the CPSM-tortuosity model and establish it as a reliable predictive tool, various applications should be implemented. Several of them are presented in the present communication.

It is of interest to note from Table 2 that τ_{CPSM} values for MCM-41 novel mesoporous materials (e.g., Wu et al.[14] and Ravikovitch et al.[15]) approach close to unity, $\tau_{CPSM} = 1.12-1.13$. Such low tortuosity factors were obtained by excluding the interparticle porosity portion and are consistent with SEM micrographs obtained from MCM-41 materials showing the presence of straight circular pores.[16,17] If both intraparticle and interparticle porosity are taken into account, the following values of the chararacteristic pore diameters are valid: (i) MCM-41 data,[14] $D_{max,\ eff} = 154.5$ nm, $D_{min,eff} = 2.28$ nm, and $D_{mean} = 46.37$ nm (psd data in Figure 5); (ii) MCM-41 data,[15] $D_{max,eff} = 173.53$ nm, $D_{min,eff} = 2.56$ nm, and $D_{mean} = 40.09$ nm (psd data in ref 15); and the respective tortuosities of the catalytic materials are $\tau_{CPSM} = 1.40$ and $\tau_{CPSM} = 1.77$. Thus, the more complex structures give rise to higher tortuosity factors.

Anodic aluminum oxide film is another material that evidently exhibits a regular pore structure that should be characterized by a relatively low tortuosity factor. The application of the present theory yielded $\tau_{CPSM} = 2.60$. Low tortuosity factors, $\tau_{CPSM} = 1.33-2.79$, have been also predicted for several samples of partially dried lignite.[18] Pore tortuosity increases from $\tau_{CPSM} \approx 1$ to $\tau_{CPSM} \approx 3$ because of pore volume evolution as the drying temperature increases from 100 to 200 °C (runs 1−4, Table 2), whereas prolonged drying (i.e., 3 h) or drying above 200 °C causes a τ_{CPSM} decrease because of a pore volume decrease. From the latter observations, one can speculate that pore volume evolution is related to the formation of longer pores of an irregular cross section. Lignite drying at temperatures exceeding 200 °C or drying at 100 °C for 3 h might result in the liberation of volatile condensable oily products that can cause blocking of certain pore structure sections. The low tortuosity factors calculated for lignite samples indicate the tracing, by the nitrogen sorption method, of rather short pores that form a more or less regular pore structure.

Furthermore, high τ_{CPSM} values have been deduced for a number of commercially available HDS catalysts (Table 2). Tortuosity factors range from 2.75 to 10.07. These values compare well with those reported in the literature[1] for supported catalysts (e.g., data of ref 1, Table 1.6 and Figure 1.5). The high τ_{CPSM} values are typical of more complex pore structures. The nominal pore length parameter (N_S) included in the CPSM model is comparatively high, ranging between 3.8 and 5.8, and constitutes the main contributing factor in the calculation of the pertinent τ_{CPSM} values through eq 7. Regarding the evaluation of coefficients A and a (eq 7), special mention should be made of the tortuosity $\tau_{CPSM} = 4.90$ of the Comox 451 catalyst whose value has been taken to be equal to that provided by the catalyst supplier.

An additional independent indication for the presence of a complex pore structure of HDS catalysts is obtained from mercury porosimetry (MP) intrusion−extrusion measurements. MP hysteresis data for these catalysts are presented in Figure 6. The amount of Hg trapped in the pores upon the termination of the retraction process is plotted against the corresponding tortuosity τ_{CPSM} values (Figure 7). This figure shows that the amount of Hg trapped increases proportionally with τ_{CPSM}. The extrapolation of the fitted curve for higher τ_{CPSM} values predicts that the relative amount of entrapped mercury asymptotically approaches unity, e.g., 100% entrapment of mercury. A correlation of ultimate mercury entrapment with the respective τ_{CPSM} values was developed as follows:

$$V_T = 1 - \frac{4.996}{1 + \exp[(\tau_{CPSM} + 5.8032)/4.6242]} \quad (8)$$

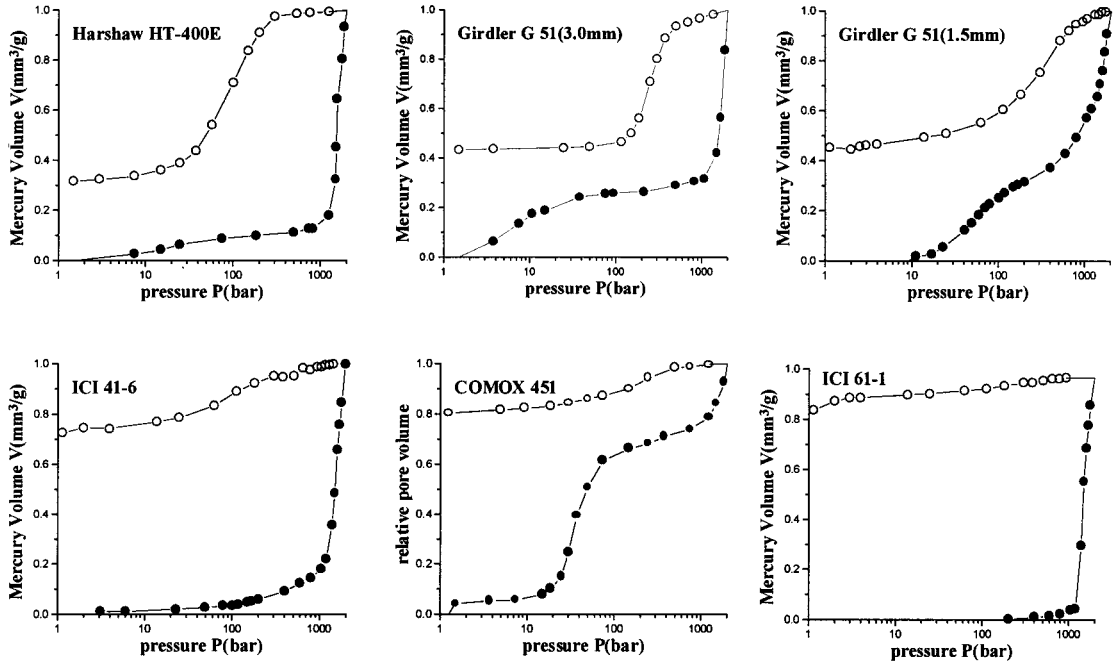

Figure 6. Experimental data of mercury porosimetry hysteresis loop for six HDS catalysts. The relevant nitrogen sorption data are presented in Figure 4. Solid symbols (●), mercury penetration data. Open symbols (○), mercury retraction data.

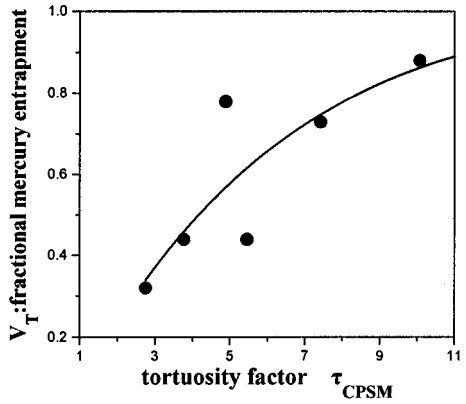

Figure 7. Relating tortuosity factor with the ultimate mercury entrapment (data from Figure 5). Data regression (solid line) by using the following correlation: $V_T = 1 - 4.996/[1 + \exp((\tau_{CPSM} + 5.8032)/4.6242)]$.

As reported in ref 11, the CPSM-mercury model predicts final entrapment that is dependent upon the intrinsic psd parameters (i.e., b, D_{min}, and D_{max}) as these values control the critical pore constriction ratio (D_{j+1}/D_j) of adjacent pore segments of a corrugated pore. For a wide pore size range, $D_{max} - D_{min}$, the pore constriction ratio is large, and according to the CPSM-mercury theory, the respective probability for mercury entrapment increases. Furthermore, intrinsic psd skewness toward D_{min} (i.e., for negative values of b if a BSD type distribution is considered) favors mercury entrapment.

The present theory has been also applied to hysteresis loops of type H_2 (IUPAC). A theoretical case (a) and an experimental one (b), reproduced from literature data,[19] are presented in Figure 8. Evidently these loops are characterized by a high N_S value (i.e., $N_S = 30-60$). A tortuosity factor of $\tau_{CPSM} = 6.6$ has been assigned to the experimental loop and aids in the evaluation of parameters A and a of eq 3. Such a tortuosity value is typical of Vycor porous glass according to ref 1. A tortuosity factor $\tau_{CPSM} = 5.89$ is deduced for the theoretical example of an H_2-type loop.[9]

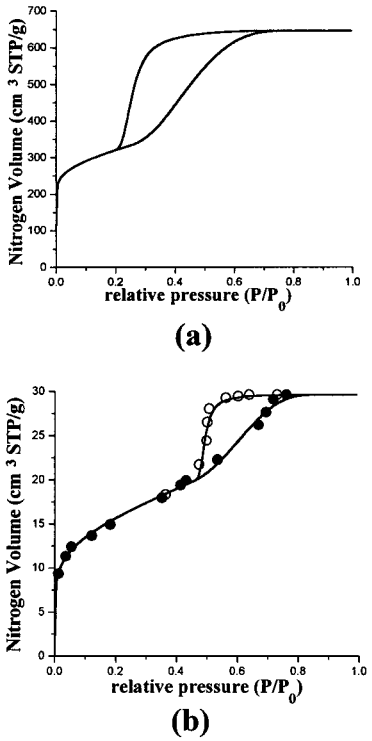

Figure 8. Nitrogen sorption hysteresis loops examples of type H_2 (IUPAC). (a) A theoretical loop (CPSM parameters: $N_S = 30$, $P_{ce}/P_0 = 0.25$, $P/P_{0max} = 0.993$, $b = -400$, $\cos\theta_c = 0.8$, $\cos\theta_h = 1.0$, $m = 0$, $n = 0.35$). (b) Experimental points[19] reproduced from Figure 3.2 of Gregg and Sing, 1982. Solid line, CPSM fitting (CPSM parameters: $N_S = 60$, $P_{ce}/P_0 = 0.46$, $P/P_{0max} = 0.99$, $b = -200$, $\cos\theta_c = \cos\theta_h = 0.38$, $m = 0.09$, $n = 0.40$).

Conclusions

Nitrogen sorption hysteresis data can be exploited for the prediction of tortuosity factors of various mesoporous materials. The evaluation of tortuosity factors based on nitrogen sorption data requires the use of a pore structure model that quantifies pore structure networking effects and accounts for pore geometry

characterization. The CPSM model is a suitable model for evaluations of tortuosity factors of various mesoporous materials.

The correlation proposed in this work enables the evaluation of low tortuosity factors (i.e., between 1 and 2) for porous materials that evidently contain pores with a more or less cylindrical geometry.

Additionally, the theory introduced in this work predicts tortuosity factors for supported catalysts that fall in the range of tortuosity values obtained by independent diffusion measurements on samples of similar materials.

The tortuosity factor of HDS catalysts, as predicted by the CPSM model, is a measure of pore structure complexity and was found to be in reasonably good agreement with mercury porosimetry ultimate entrapment observations.

The present theory yields realistic predictions of tortuosity factors for materials exhibiting an H_2-type gas sorption hysteresis (e.g., Vycor glass) that are associated with high nominal pore length values (i.e., $N_S = 30-60$).

To establish the proposed theory as an independent method for predicting tortuosity factors without resorting to diffusion measurements, the CPSM model should be further tested by carrying out combined studies involving nitrogen sorption porosimetry and tortuosity evaluation via a CPSM simulation of diffusion measurements.

Nomenclature

a = proportionality constant of eq 3
A = proportionality constant of eq 3
d_s = critical molecular diameter of solute
d_p = pore diameter
D = pore diameter (nm)
D_b = binary molecular diffusion coefficient (eq 1)
D_e = effective diffusion coefficient (effective diffusivity, eq 1)
D_C, D_h = diameter of pore filled with condensate through a cylindrical or a hemispherical liquid/vapor interface shape (nm)
D_K = Kelvin core diameter (nm)
D_{min}, D_{max} = minimum and maximum pore diameters detected by nitrogen condensation (nm)
$D_{min,eff}$, $D_{max,eff}$ = defined by eq 6
D_{mean} = mean pore diameter as predicted by the intrinsic pore size distribution
$f_r(b_r;D)$ = component pore number distribution function (eq I-7) of BSD type used in the synthesis of $F(D)$
$F(D)$ = intrinsic pore number distribution density function, as defined by eq I-6
$F_V(D)$ = intrinsic pore volume distribution density function
$F(\lambda)$ = function defined in eq 1
m = exponent in eq I-1
n = multiplication factor in eq I-1
N_S = number of pore segments forming a corrugated pore (also frequency of pore cross-sectional area variation)
P/P_0 = relative gas pressure
P_j = probability for at least one liquid/vapor hemispherical interface to be adjacent to the general jth segment of a corrugated pore[9]
q = probability for a pore segment of size D_j to be within the range D_h-D_{max}[7]
t = thickness of physically adsorbed nitrogen multilayer (nm)
V_{ads} = relative saturation during capillary condensation
V_{der} = relative pore volume evacuated by desorbed−evaporated nitrogen (eq I-5)
V_p = specific pore volume (cm^3/g)
V_{sr} = relative saturation during capillary evaporation ($1 - V_{der}$)
V_T = fractional mercury entrapment at the end of mercury retraction process
w_i = relative weight of the ith BSD function used in the synthesis of a multimodal psd

Acronyms

CPSM = corrugated pore structure model
BSD = bell-shaped distribution function, $(D - D_{min})(D - D_{max}) \exp(bD)$
HDS = hydrodesulfurization
MCM-41 = mobil catalytic material (novel mesoporous materials)[16]
psd = pore size distribution

Greek Letters

ϵ = porosity (cm^3 of voids/cm^3 of particles)
θ_C, θ_h = liquid nitrogen contact angle for cylindrical and hemispherical liquid nitrogen meniscus, respectively.
λ = ratio of critical molecular diameter to pore diameter ($\lambda = d_s/d_p$), eq 1
τ = tortuosity factor as defined by eq 1 (dimensionless)
τ_{CPSM} = tortuosity factor as defined by eq 3 (dimensionless)

Appendix

Adsorbed Nitrogen Multilayer Thickness. A modified Halsey equation has been tested[10] in various applications concerning the curve fitting of experimental materials and is also used in the present work.

$$t = n\left[\frac{5}{\ln(P_o/P)}\right]^{1/3}(P/P_o)^m \qquad \text{(I-1)}$$

where $n = 3.5-4.3$ and $m = 0-0.1$.

The Kelvin Equation. The version of the Kelvin equation to be used in the hysteresis loop simulations by means of the CPSM model is shown in eq I-2.[9]

$$D_K = \frac{1.906}{\ln(P_0/P)}\cos\theta \qquad \text{(I-2)}$$

where D_K is the Kelvin diameter (nm) and θ is the nitrogen liquid/vapor interface contact angle ($\cos\theta = 0.5$ for a cylindrical interface geometry, $\cos\theta = 1.0$ for a hemispherical interface geometry).

Generally, $\cos\theta$ can assume values even lower than $\cos\theta = 0.5$, associated with an arbitrary interface geometry, especially when applied to microporous materials.

Simulation of the Adsorption−Capillary Evaporation Isotherm Using the CPSM Model. The relative volume of gas been adsorbed V_{ads} at a specified relative pressure can be computed via eq I-3.

$$V_{ads} = [1/\int_{D_{min}}^{D_{max}} D^2F(D)\,dD]\left[4t\int_{D_h}^{D_{max}}(D-t)F(D)\,dD + \int_{D_{min}}^{D_C} D^2F(D)\,dD + \int_{D_C}^{D_h} D^2F(D)\,dD\left(\frac{1}{N_S}\sum_{j=1}^{j=N_S}(P_j)\right) + 4t\int_{D_C}^{D_h}(D-t)F(D)\,dD\left(\frac{1}{N_S}\sum_{j=1}^{j=N_S}(1-P_j)\right)\right] \qquad \text{(I-3)}$$

Simulation of the Desorption−Capillary Evaporation Isotherm Using the CPSM Model. The relative amount of nitrogen evaporated and/or desorbed, V_{der}, as a function of the relative gas pressure can be evaluated via eq I-5, and the fraction of the pore volume, V_{sr}, saturated with nitrogen is given by eq I-4.

$$V_{sr} = 1 - V_{der} \tag{I-4}$$

$$V_{der} = \int_{D_h}^{D_{max}} (D - 2t)^2 F(D)\, dD \times \left(\frac{2}{N_S}\frac{1 - q^{N_S}}{1 - q} - q^{N_S - 1}\right) \Big/ \int_{D_{min}}^{D_{max}} D^2 F(D)\, dD \tag{I-5}$$

Proof of eqs I-3 and I-5 is presented elsewhere.[9]

Intrinsic Pore Segment Number Distribution Function. The normalized $F(D)$ in its general form (i.e., composed of n unimodal psds) reads

$$F(D) = \sum_{r=1}^{r=n}\left(\frac{w_r}{R_r}\right)\frac{f_r(b_r;D)}{\Phi_r} \Big/ \sum_{r=1}^{r=n}\left(\frac{w_r}{R_r}\right) \tag{I-6}$$

where w_r is the weight of a unimodal psd, $\sum_{r=1}^{r=n} w_r = 1$

$$f_r(b_r;D) = (D - D_{min})(D - D_{max}) \exp(bD) \tag{I-7}$$

$$\Phi_r = \int_{D_{min}}^{D_{max}} (D - D_{min})(D - D_{max}) \exp(bD)\, dD \tag{I-8}$$

where Φ_r is the normalization factor of $f_r(b_r;D)$ and $R_r = \int_{D_{min}}^{D_{max}} D^2(f_r/\Phi_r)\, dD$ is the normalization factor of each one of the pore volume distributions composing the overall pore volume distribution.

Literature Cited

(1) Satterfield, C. N. *Mass Transfer in Heterogeneous Catalysis*; M.I.T. Press: Cambridge, MA, 1970.

(2) Furimsky, E.; Massoth, F. E. Deactivation of Hydroprocessing Catalysts. *Catal. Today* **1999**, *52*, 381−495.

(3) Petersen, E. E. Diffusion in a Pore of Varying Cross Section. *AIChE. J.* **1958**, *3*, 343−345.

(4) Michaels, A. S. Diffusion in a Pore of Irregular Cross Section−A Simplified Treatment. *AIChE J.* **1959**, *4*, 270−271.

(5) Beck, R. E.; Schultz, J. S. Hindered Diffusion in Microporous Membranes with Known Pore Geometry. *Science* **1970**, *170*, 1302−1305.

(6) Satterfield, C. N.; Colton C. K.; Pitcher, W. H. Restricted Diffusion in Liquids within Fine Pores. *AIChE J.* **1973**, *19*, 628−635.

(7) Chantong, A.; Massoth, F. E. Restricted Diffusion in Aluminas. *AIChE J.* **1983**, *29*, 725−731.

(8) Carniglia, S. C. Construction of the Tortuosity Factor from Porosimetry. *J. Catal.* **1986**, *102*, 401−418.

(9) Androutsopoulos, G. P.; Salmas, C. E. A New Model for Capillary Condensation−Evaporation Hysteresis Based on a Random Corrugated Pore Structure Concept: Prediction of Intrinsic Pore Size Distributions. 1. Model Formulation. *Ind. Eng. Chem. Res.* **2000**, *39*, 3747−3763.

(10) Androutsopoulos, G. P.; Salmas, C. E., A New Model for Capillary Condensation-Evaporation Hysteresis based on a Random Corrugated Pore Structure Concept: Prediction of Intrinsic Pore Size Distributions. 2. Model Application. *Ind. Eng. Chem. Res.* **2000**, *39*, 3764−3777.

(11) Androutsopoulos, G. P.; Salmas, C. E. A Simplified Model for Mercury Porosimetry Hysteresis. *Chem. Eng. Commun.* **1999**, *176*, 1−42.

(12) Androutsopoulos, G. P.; Salmas, C. E. Tomography of Macro−Meso-Pore Structure, Based on Mercury Porosimetry Hysteresis Loop Scanning. Part I: MP Hysteresis Loop Scanning along the Overall Penetration Line. *Chem. Eng. Commun.* **2000**, *181*, 137−177.

(13) Androutsopoulos, G. P.; Salmas, C. E. Tomography of Macro−Meso-Pore Structure Based on Mercury Porosimetry Hysteresis Loop Scanning. Part II: MP Hysteresis Loop Scanning along the Overall Retraction Line. *Chem. Eng. Commun.* **2000**, *181*, 179−202.

(14) Wu, C. N.; Tsai, T. S.; Liao, C. N.; Chao, K. J. Controlling Pore Size Distributions of MCM-41 by Direct Synthesis. *Microporous Mater.* **1996**, *7*, 173−185.

(15) Ravikovitch, P. I.; Haller, G. L.; Neimark, A. V. Density Functional Theory for Calculating Pore Size Distributions. Pore Structure of Nanoporous Catalysts. *Adv. Colloid Interface Sci.* **1998**, *76−77*, 203−226.

(16) Beck, J. S.; Vartuli, J. C.; Roth, W. J.; Leonowitcz, M. E.; Kresge, C. T.; Scmitt, K. D.; Chu, C. T-W.; Olson, D. H.; Sheppard, E. W.; McCullen, S. B.; Higgins, J. B.; Schlenker J. L. A New Family of Mesoporous Molecular Sieves Prepared with Liquid Crystal Templates. *J. Am. Chem. Soc.* **1992**, *114*, 10834−10843.

(17) Rouquerol, F.; Rouquerol, J.; Sing, K. *Adsorption by Powders and Porous Solids*; Academic Press: New York, 1999.

(18) Salmas C. E.; Tsetsekou A. H.; Hatzilyberis K. S.; Androutsopoulos, G. P. Lignite Meso-Pore Structure Evolution During Drying: Effect of Temperature and Heating Time. *Drying Technol.*, manuscript accepted for publication.

(19) Emmett, P. H.; Cines, M. *J. Phys. Chem.* **1947**, *56*, 735 (as quoted in Gregg, S. J.; Sing, K. S. W. *Adsorption Surface Area and Porosity*; Academic Press: New York, 1982).

Received for review June 29, 2000
Revised manuscript received October 17, 2000
Accepted October 20, 2000

IE000626Y